2022 IEEE International Symposium on Circuits and Systems (ISCAS) | 978-1-6654-8485-5/22/$31.00 ©2022 IEEE | DOI: 10.1109/ISCAS48785.2022.9937487

System-Level Modeling and Design of a Temperature Compensated CMOS MEMS Thermal Flow Sensor

Zhijuan Li[1], Zetao Fang[1], Bo Wang[2], Moaaz Ahmed[2], Xiaofang Pan[1], Su-Ting Han[1], Xiaojin Zhao[1], Wei Xu[1,*]
[1]College of Electronics and Information Engineering, Shenzhen University, Shenzhen, China
[2]College of Science and Engineering, Hamad Bin Khalifa University, Doha, Qatar
*Email: weixu@szu.edu.cn

Abstract—In this paper, we present a system-level model for an ambient temperature-compensated CMOS MEMS Thermal Flow (C²MTF) sensor. The system-level model is first validated by a computational fluid dynamics (CFD) model and is further used for a fully coupled simulation between the microstructure, heat transfer, and interface circuits. Correspondingly, a monolithically integrated C²MTF sensor is designed and optimized using a 0.18 µm 1P6M CMOS MEMS technology. The designed System on Chip (SoC) C²MTF sensor has a flow range of -10~10 m/s, and its highest sensitivity is 0.274 V/(m/s) with a system power consumption of less than 3.6 mW. In comparison with the more than 50% output drift for the uncompensated counterpart, the output drift of the designed C²MTF sensor is reduced to 7% under an ambient temperature of 0~50 °C. In addition, based on the proposed system-level model, the additional optimizations show that the output drift can be greatly reduced to 0.5%, by arranging another on-chip overheated temperature-regulating resistor R_c in the future, delicately.

Keywords—system-level model, CMOS MEMS thermal flow sensor, temperature compensation, SoC, monolithic integration.

I. Introduction

High-precision flow sensors are essential in both industrial and biomedical applications [1, 2]. With the development of semiconductor technology, flow sensors can be integrated on a tiny chip by using CMOS MEMS technology, thereby greatly reducing the sensor footprint, noise, and power consumption [3]. The majority of micro flow sensors can be classified as either thermal or non-thermal. In particular, the research on micro thermal flow sensors has extensively focused on various operating principles [4] and application scenarios [1], due to their structural, electronic simplicity, and capability of CMOS integration [5]. However, thermal flow sensors usually suffer inconsistent signal output due to ambient temperature variation. To enable these thermal flow sensors to be applied in the changing ambient environments, such as the medical ventilator systems, huge time-consuming calibration is usually needed over the specified flow range and operating temperature.

Several ambient temperature-compensated micro thermal flow sensors [6-8] have been reported, while most of them were developed based on hot wire or hot film anemometer principle and the fabrication process was not compatible with CMOS technology. Xu et al. reported a low-cost ambient temperature compensated micro calorimetric flow sensor using a 0.35 µm 2P4M CMOS MEMS technology [9]. However, in their work, the whole sensor system is still not fully integrated, and the temperature drift caused by the off-chip interface circuit is ignored. To the best of our knowledge,

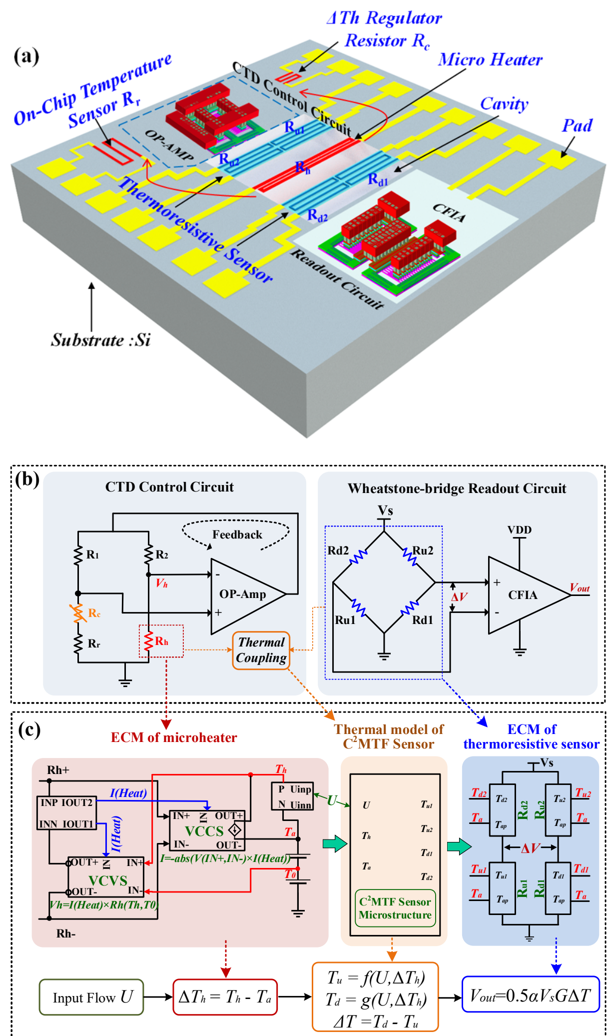

Fig. 1. (a) Schematic of an integrated System-on-Chip (SoC) flow sensor using 0.18 µm 1P6M CMOS MEMS technology, (b) Interface circuit for C²MTF sensor: (left) constant temperature difference (CTD) control circuit with the on-chip reference temperature sensor R_r and the overheated temperature-regulating resistor R_c; (right) Wheatstone bridge readout circuit with Current Feedback Instrument Amplifier (CFIA); note that all components are designed on-chip, while R_c can be arranged either on-chip or off-chip. (c) The equivalent circuit model (ECM) for microheater and themoresistive sensors; note that the two ECM models are coupled with a linear thermal model to form a system-level model.

there is no satisfactory system-level model to predict the performance of the SoC sensor and overcome the challenge in the complexity of the coupled mechanical, thermal, and electrical analysis. Such a system-level model will be very critical for designing a robust and temperature compensated CMOS MEMS thermal flow sensor.

In this paper, we proposed a non-linear system-level model for the design of a temperature-compensated CMOS-MEMS Thermal Flow (C^2MTF) sensor, as shown in Fig. 1. Two precise on-chip analog circuits, including one constant temperature difference (CTD) control circuit and one low noise current feedback instrument amplifier (CFIA) readout circuit, are implemented as the interface of the C^2MTF sensor, as shown in Fig. 1(a). With the validated system-level model (Fig. 1(c)), the effect of ambient temperature on this SoC flow sensor is investigated. Then, the design of the C^2MTF sensor is introduced, and further guidance for a smart sensor system with extremely low temperature drifting (0.5%) is revealed.

II. Concept and Circuit Implementation

The C^2MTF sensor is arranged with two pairs of symmetric upstream and downstream thermistors R_u and R_d at the same location to form a Wheatstone bridge circuit. A microheater R_h is placed in the center and maintained with a constant temperature of 50 °C by a constant temperature difference (CTD) control circuit, as shown in Fig. 1(a). In the presence of fluid flow U, the temperature distribution around R_h is distorted, causing a temperature difference output of $\Delta T = T_d - T_u$ through heat transfer. The Wheatstone bridge converts ΔT to an electrical signal of ΔV and amplifies it through a low-noise current feedback instrument amplifier (CFIA). Thus, the final sensor system output of V_{out} can be related to the input flow velocity U. Note, the microstructure of the C^2MTF sensor will be released by a home-developed post-CMOS process [10], and a bottom cavity will be formed to reduce the sensor power by frontside oxide and silicon etching, as shown in Fig. 1(a).

A. CTD Control Circuit

The left part of Fig. 1(b) is the CTD control circuit, which is used to keep the microheater R_h working at a constant temperature difference with respect to the ambient temperature T_a. The circuit is mainly composed of five resistors in a Wheatstone bridge and a dedicated on-chip operational amplifier. The ratio of R_1/R_2 and $(R_r + R_c)/R_h$ is designated as 5 to ensure most of the power is consumed by R_h. The microheater R_h and the on-chip reference temperature sensor R_r are made by P+ poly-Si, which has a good linear temperature coefficient of resistance (TCR) α of 0.003. By configuring the regulation resistor $R_c = \alpha R_{r0}\Delta T_h$ (where R_{r0} is the value of R_r at the reference temperature T_0 = 25 °C, ΔT_h is the overheated temperature regulated by R_c), the negative feedback loop around the operational amplifier guarantees V+ = V−, which ensures the R_h works on a constant ΔT_h under different input flow velocities and is not affected by T_a. In addition, to ensure an accurately controlled CTD mode for the SoC flow sensor, the operational amplifier is designed with a large gain of 97 dB and also a strong current drive capability of more than 52.8 mA.

B. Readout Circuit

Since the voltage output ΔV of the Wheatstone bridge is usually in the mV level, a CFIA is designed as the back-end readout circuit with signal amplification. Fig. 2 is a block diagram of the three-stage CFIA, where $G_{m,\,in}$ and $G_{m,\,fb}$ is the input and feedback transconductance, respectively, and they are used to convert the output and feedback voltages into the current. The input stage uses PMOS input pair folded-cascade to meet the near-ground sensing capability and low flicker noise characteristics. The CFIA is chopped at 50 kHz to eliminate low-frequency noise. A low pass filter helps to remove the chopping ripple at the output. Fig. 3 shows the input-referred noise spectral density of the closed-loop CFIA, the thermal noise floor is 4.32 nV/√HZ. Moreover, the CFIA has a closed-loop gain of 200, a high CMRR of greater than 163 dB, and power consumption as low as 1.49 mW. Such a precise amplifier (CFIA) can serve as a good interface readout circuit for the C^2MTF sensor.

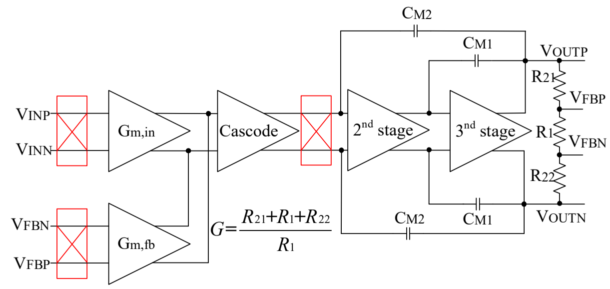

Fig. 2. Block diagram of implemented chopped CFIA and the gain is designed to be 200.

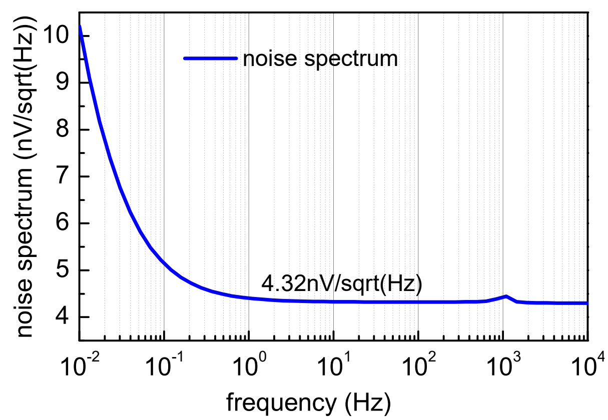

Fig. 3. The simulated input-referred noise spectrum shows the post-chopped flicker noise corner is around 300 mHz and the thermal noise floor is around 4.32 nV/√Hz.

III. System-level Model

To realize a system-level simulation of the C^2MTF sensor, two important equivalent circuit models (ECM) should be established for the interface circuit, one is the CTD feedback circuit for the microheater, and another is Wheatstone bridge circuit for the themoresistive sensors, as shown in Fig. 1(c). The Verilog-A is used for the analog behavior modeling of microheater and upstream and downstream thermistors. Coupled with an analytical thermal model, the whole flow sensor system is built in a Cadence Virtuoso platform. Finally, the Spectre simulator is used to realize the system-level simulation and optimization of the C^2MTF sensor.

A. ECM of the microheater

For the microheater controlled by a CTD circuit, a force-thermal-electric coupling simulation is required. Therefore, the modified King's law and energy balance are adopted in the establishment of ECM for microheater, as follows:

$$(A+BU^n)(T_h-T_a)+\rho_h C_h V_h \frac{dT_h}{d\tau}=I^2R_h \quad (1)$$

where A is the heat conduction loss, BU^n is the heat convection loss within the thermal boundary layer, n depends on the sensor structure, which is 0.5742 in this design. Note, the parameters A, B, and n can be fitted from the power loss in a followed analytical thermal model of (2). ρ_h is the density of the microheater, C_h is the heat capacity, V_h is the volume. Therefore, the ECM of the microheater in Fig. 1(c) can be obtained. Among them, VCCS is a voltage-controlled current source, which converts the voltage and current signals of the microheater into heating power. VCVS is a voltage source controlled voltage source, which converts the heating temperature T_h into a voltage signal V_h.

B. Analytical Thermal Model

The analytical thermal model of the micro calorimetric flow sensor can be found in [9] and is introduced as follows:

$$(k_s t+\frac{1}{2}k_m(\delta_t+h)\frac{d^2T(x)}{dx^2})-\rho_m C_{pm} U\beta_i \frac{dT(x)}{dx}-(\frac{k_m}{\delta_t}+\frac{k_m}{h})T(x)=0 \quad (2)$$

the parameters of k_m, ρ_m, C_{pm}, and δ_t are all related to temperature, and the corresponding formula can be obtained in [9, 12]. Therefore, the analytical solution of the temperature distribution $T(x)$ of a C^2MTF sensor in the streamwise (x) direction can be obtained, where the calculated upstream and downstream temperature T_u and T_d can be transferred to ECM of thermistors.

C. ECM of thermistors

The ECM of the thermistor can be simply calculated as a function of temperature:

$$R=R_0(1+\alpha(T(x)+T_a-T_0)) \quad (3)$$

where R_0 is the resistance of the thermistor at the reference temperature of $T_0=25$ °C. $T(x)$ is the analytical solution of (2). Therefore, combining (2) and (3), we can easily construct the ECM of a thermistor, as shown in Fig. 1(c).

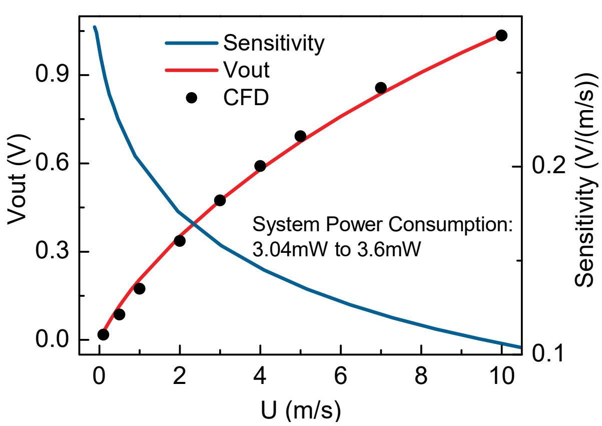

Fig. 4. Comparison of C^2MTF sensor output between system-level model and CFD model at the ambient temperature of 25 °C, and fitting factor is 2.3. The system power is smaller than 3.6 mW and the maximum sensitivity is 0.274 V/(m/s).

IV. Result and Discussion

A. Simulation result of System-level model

Fig. 4 shows the sensor output from the system-level model and its comparison with the 2D computational fluid dynamics (CFD) model. It can be seen that the system-level model is in good agreement with the CFD model with a simple fitting factor of 2.3. Fig. 4 also shows the predicted sensitivity of the C^2MTF sensor. The maximum sensitivity is 0.274 V/(m/s), which proves that the C^2MTF sensor has high sensitivity in the low flow region. The results show that there is a trade-off between the sensitivity and output of the C^2MTF sensor. Moreover, the integrated SoC flow sensor has a very low system power consumption of 3.04~3.6 mW in the flow range of 0~10 m/s.

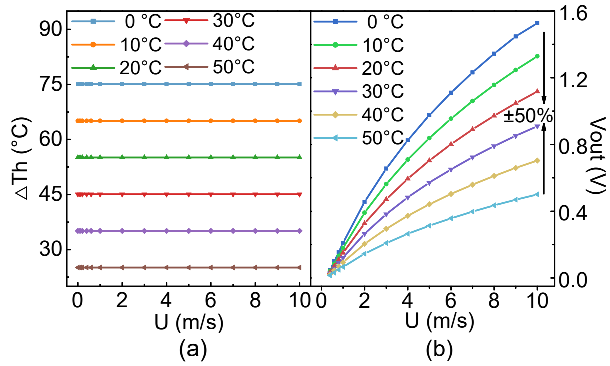

Fig. 5. Simulation results of the non-compensated flow sensor under the ambient temperature of 0~50 °C and flow range of 0~10 m/s: (a) The predicted overheated temperature ΔT_h correspondingly drops from 75 °C to 25 °C. (b) The output voltage of the flow sensor drops sharply with a variation of more than 50%.

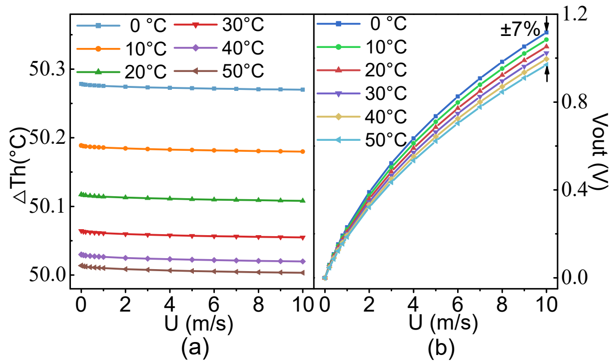

Fig. 6. The simulated C^2MTF sensor output under different ambient temperatures T_a: (a) ΔT_h is slightly decreased from 50.27 °C to 50.01 °C with a variation of less than 0.53%, (b) The predicted system output of C^2MTF sensor has a variation of ±7% when referring to the room temperature of 25 °C.

B. Comparison with and without CTD circuit

As displayed in Fig. 5, by setting the microheater working in a constant temperature (CT) mode, the system-level model simulated ΔT_h correspondingly drops from 75 °C to 25 °C when the ambient temperature changes from 0 °C to 50 °C. Consequently, the output voltage of the flow sensor system dramatically decreased, with a change of up to 50%. While by configuring the microheater in the CTD mode, as shown in Fig. 6(a), ΔT_h is almost maintained at a constant value of 50 °C (variation < 0.53%.) under different input flow velocities and ambient temperature. The simulated output of the C^2MTF sensor system is only slightly reduced (±7%) with the ambient temperature range from 0 °C to 50 °C, as shown in Fig. 6(b). The model simulation results illustrate that the proposed interface circuit can effectively suppress the temperature drifting.

C. Optimization of Interface Circuit

The system-level model is further leveraged to study the impact of ambient temperature on the C²MTF sensor performance. Accordingly, an overheated temperature-regulating resistor R_c (either on-chip or off-chip) with positive TCR is proposed with automatically adjusted ΔT_h for output drifting reduction. As shown in Fig. 7(a), by configuring a positive TCR R_c in the system, ΔT_h slightly rises from 46.7 °C to 54.22 °C when T_a changes from 0 °C to 50 °C. In this way, the decreased sensor output in Fig. 6(b), can be automatically compensated with the increased ΔT_h. Based on the system-level model simulation, our optimized C²MTF sensor shows an excellent temperature insensitivity, while the output variation is as small as 0.5%, as shown in Fig. 7(b).

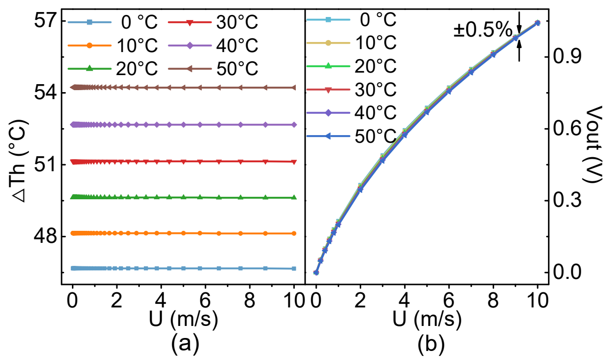

Fig. 7. The proposed on-chip overheated temperature-regulating resistor for the automatically increased ΔT_h. (a) Under an ambient temperature T_a of 0 °C to 50 °C, ΔT_h is automatically raised from 46.7 °C to 54.22 °C accordingly. (b) The simulated output variation of the C²MTF sensor is significantly suppressed with a variation of less than ±0.5%.

Table I summarizes our proposed C²MTF sensor performance and compares it with the prior of art. Our C²MTF sensor is fully integrated with a flow range of -10~10 m/s, a system power of < 3.6 mW, and high sensitivity of 274 mV/(m/s). Fig. 8 is the optical graph of the designed C²MTF sensor in a SMIC 0.18 μm 1P6M CMOS MEMS technology, note that an offset zeroing circuit is also configured for CFIA.

TABLE I. Performance Comparison Between the Reported Thermal Flow Sensor and Our C²MTF Sensor

Reference	Flow Range m/s	Power mW	S V/(m/s)	TC	MI
Nebhen[12], *	0~26	3[b]	0.117	N/A	YES
Bruschi[13], *	-3.33~3.33	4[b]	0.0023	N/A	YES
Dong[14], *	0.5~40	2~452.6[b]	0.0079	N/A	N/A
Makinwa[15], *	0.02-38	400-600[a]	N/A	N/A	YES
Mansoor [16], *	0~26	9.4[b]	0.936	N/A	N/A
Xu[9], *	-11~11	2.36~2.77[b]	0.543	YES/0.5%	N/A
This work#	**-10~10**	**3.04~3.6[a]**	**0.274**	**YES/±0.5%**	**YES**

[a] Power of sensor system, [b] Power of microheater, * Experimental results, # Simulation results, S = Sensitivity, TC = Temperature Compensation, MI = Monolithic Integration of MEMS flow sensor and interface circuit on a single chip.

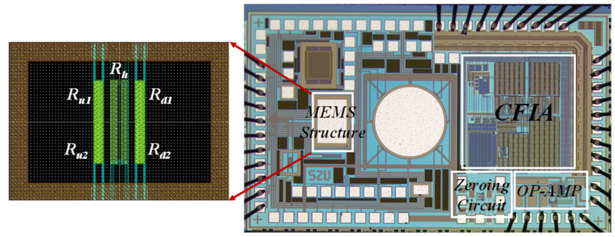

Fig. 8. The optical graph of the C²MTF sensor chip and the layout design of the microstructure. Note that the MEMS structure will be released by a home-developed post-CMOS process.

V. Conclusion

We proposed a non-linear system-level model for the design and optimization of a C²MTF sensor. The designed C²MTF sensor can sense the bi-directional flow of -10~10 m/s. The maximum power consumption of the whole sensor system is less than 3.6 mW, and the designed CFIA interface has input reference noise spectral density as low as 4.32 nV/√Hz. Under the typical application scenario with the ambient temperature range from 0 °C to 50 °C, the designed C²MTF sensor shows that it has a low output drift of ±7%. Moreover, a simple method is proposed to optimize the interface circuit with reduced temperature drifting, by arranging a positive TCR overheated temperature-regulating resistor R_c. Consequently, the output drift of the C²MTF sensor can reduce to less than ±0.5%. Therefore, this robust, high-sensitivity, low-power, and temperature-drift-inhibited C²MTF sensor will be a very promising sensing node in the medical ventilator.

Acknowledgments

Zhijuan Li and Zetao Fang contributed equally to this work.

This work was supported in part by the National Natural Science Foundation of China under Grant 52105582 and 62174111, in part by the Natural Science Foundation of Guangdong Province under Grant 2020A1515011555, in part by the High-Talent Research Funding under Grant 827-000451, in part by the Fundamental Research Foundation of Shenzhen under Grant JCYJ20210324095210030 and JCYJ20190808151819049, and in part by the Open Foundation of The State Key Laboratory of Digital Manufacturing Equipment and Technology under Grant DMETKF2021016.

References

[1] E. Fatemeh, A. Shohreh, A. Razmjou, Y. Orooji, A. Kottapalli, and M. E. Warkiani, "Design and applications of MEMS flow sensors: A review," Sensors and Actuators A: Physical, vol. 295, pp. 483-502, Aug. 2019.

[2] S. Silvestri and E. Schena, "Micromachined Flow Sensors in Biomedical Applications," Micromachines, vol. 3, no. 2, pp. 225-243, March. 2012.

[3] E. Yoon and K. D. Wise, "An integrated mass flow sensor with on-chip CMOS interface circuitry," in IEEE Transactions on Electron Devices, vol. 39, no. 6, pp. 1376-1386, June. 1992.

[4] N. T. Nguyen, "Micromachined flow sensors—A review," Flow Measurement and Instrumentation, vol. 8, no. 1, pp. 7–16, Mar. 1997.

[5] M. Ahmed, W. Xu, S. Mohamad, F. Boussaid, Y. K. Lee, and A. Bermak, "Fully Integrated Bidirectional CMOS-MEMS Flow Sensor With Low Power Pulse Operation," in IEEE Sensors Journal, vol. 19, no. 9, pp. 3415-3424, May. 2019.

[6] T. Kei, S. Isao, and I. Koichi, "Simple temperature compensation of thermal air-flow sensor," Sensors and Actuators A: Physical, vol. 57, no. 3, pp. 197-201, Dec. 1996.

[7] H. Lundström, M. Sandberg, and B. Mosfegh, “Temperature dependence of convective heat transfer from fine wires in air: A comprehensive experimental investigation with application to temperature compensation in hot-wire anemometry,” Experimental Thermal and Fluid Science, vol. 32, no. 2, pp. 315-319, Nov. 2007.

[8] C. Sosna, R. Buchner, and W. Lang, “A Temperature Compensation Circuit for Thermal Flow Sensors Operated in Constant-Temperature-Difference Mode,” in IEEE Transactions on Instrumentation and Measurement, vol. 59, no. 6, pp. 1715-1721, June. 2010.

[9] W. Xu, S. Ma, X. Wang, Y. Chiu, and Y. K. Lee, “A CMOS-MEMS Thermoresistive Micro Calorimetric Flow Sensor With Temperature Compensation,” in Journal of Microelectromechanical Systems, vol. 28, no. 5, pp. 841-849, Oct. 2019.

[10] W. Xu, X. Wang, Z. Ke, and Y. K. Lee, “Bidirectional CMOS-MEMS Airflow Sensor with sub-mW Power Consumption and High Sensitivity,” in IEEE Transactions on Industrial Electronics, Mar. 2021.

[11] P. T. Tsilingiris, “Thermophysical and transport properties of humid air at temperature range between 0 and 100 degrees C,” Energy Convers. Manage, vol. 49, no. 5, pp. 1098–1110, May. 2008.

[12] J. Nebhen, K. Alnowaiser, and S. Mansouri, “Constant Temperature Anemometer with Self-Calibration Closed Loop Circuit,” Applied Sciences, vol. 10, no. 10, pp. 3405, Apr. 2020.

[13] P. Bruschi, M. Dei, and M. Piotto, “A single chip, double channel thermal flow meter,” Microsyst. Technol, vol. 15, no. 8, pp. 1179–1186, Aug. 2009.

[14] Z. Dong, J. Chen, Y. Qin, M. Qin, and Q. -A. Huang, “Fabrication of a micromachined two-dimensional wind sensor by Au–Au wafer bonding technology,” J. Microelectromech. Syst, vol. 21, no. 2, pp. 467–475, Apr. 2012.

[15] K. A. A. Makinwa and J. H. Huijsing, “A smart wind sensor using thermal sigma-delta modulation techniques,” Sensors and Actuators A: Physical, vol. 97, pp. 15–20, Apr. 2002.

[16] M. Mansoor, I. Haneef, S. Akhtar, M. A. Rafiq, A. D. Luca, S. Z. Ali, and F. Udrea, “An SOI CMOS-based multi-sensor MEMS chip for fluidic applications,” Sensors, vol. 16, no. 11, pp. 1608, Nov. 2016.